JPG Journal of Petroleum Geology

STRATIGRAPHIC FRAMEWORK FOR ZECHSTEIN CARBONATES ON THE UTSIRA HIGH, NORWEGIAN NORTH SEA

Lars Stemmerik[1,2]*, Kasper H. Blinkenberg[1], Ingrid P. Gianotten[3], Malcolm S.W. Hodgskiss[4], Aivo Lepland[4], Päärn Paiste[5], Israel Polonio[3], Nicholas M.W. Roberts[6] and Niels Rameil[3]

The preserved Zechstein succession on the Utsira High in the NE part of the Norwegian North Sea is 25-100 m thick and is dominated by shelf carbonates. Internal subdivision of the succession is based on the recognition of key surfaces in petrophysical logs and cores, and suggests that the carbonates mainly consist of ZS2 and ZS3 deposits and that younger ZS4 and ZS5 deposits are only locally preserved. The carbonates have undergone early, syn-depositional dolomitization followed by later dolomite recrystallization and calcitization. Calcitization, interpreted as dedolomitization, is restricted to the upper part of the ZS3 carbonate unit and based on U/Pb dating took place during the Triassic, with a later phase of recrystallization linked to mid-Jurassic uplift. Both dedolomitization and dolomite recrystallization relate to fresh-water infiltration with the resetting of δO^{18} values prior to the Late Jurassic drowning of the Utsira High. The reservoir quality of the carbonates is directly linked to post-depositional meteoric diagenesis, and the best reservoir properties are recorded in intervals dominated by recrystallized dolomites in ZS2 and lower ZS3 carbonates. Dedolomitization significantly reduced porosity in the upper ZS3 carbonates.

INTRODUCTION

The Avaldsnes and Lille Prinsen discoveries (later renamed Johan Sverdrup and Symra, respectively) in the Norwegian North Sea have resulted in intense drilling activity in the greater Utsira High area with many new wells penetrating down into the Zechstein (Fig. 1). Production at the Johan Sverdrup field is from the uppermost Triassic – Jurassic Statfjord and Viking Groups (Ottesen *et al.*, 2022). Most of the nearby fields to the NW and west, such as Ivar Aasen and Troldhaugen, produce from older Triassic sediments and weathered and fractured basement (Riber *et al.*, 2015), whereas Upper Permian Zechstein dolomites form an important part of the reservoir in the Symra discovery.

The sedimentary record preserved on the Utsira High is greatly reduced due to multiple events of rifting, uplift and erosion (Riber *et al.*, 2015; Ottesen *et al.*, 2022), and the drilled Zechstein sediments

[1]Geological Survey of Denmark and Greenland, Øster Voldgade 10, DK-1350 Copenhagen K, Denmark.
[2]Department of Arctic Geology, University Centre in Svalbard, P.O. Box 156, N-9171, Longyearbyen, Norway.
[3]Aker BP ASA, Strandveien 4, N-1366 Lysaker, Norway.
[4]Geological Survey of Norway, Leiv Eirikssons vei 39, N-7040 Trondheim, Norway.
[5]Department of Geology, Ravila 14a, University of Tartu, Tartu, 50411, Estonia.
[6]Geochronology and Tracers Facility, British Geological Survey, Nottingham, NG12 5GG.

*Corresponding author: ls@geus.dk

Key words: Upper Permian, Zechstein Supergroup, reservoir potential, carbonate-evaporite systems, dedolomitization, U/Pb geochronology, Utsira High, Norwegian North Sea.

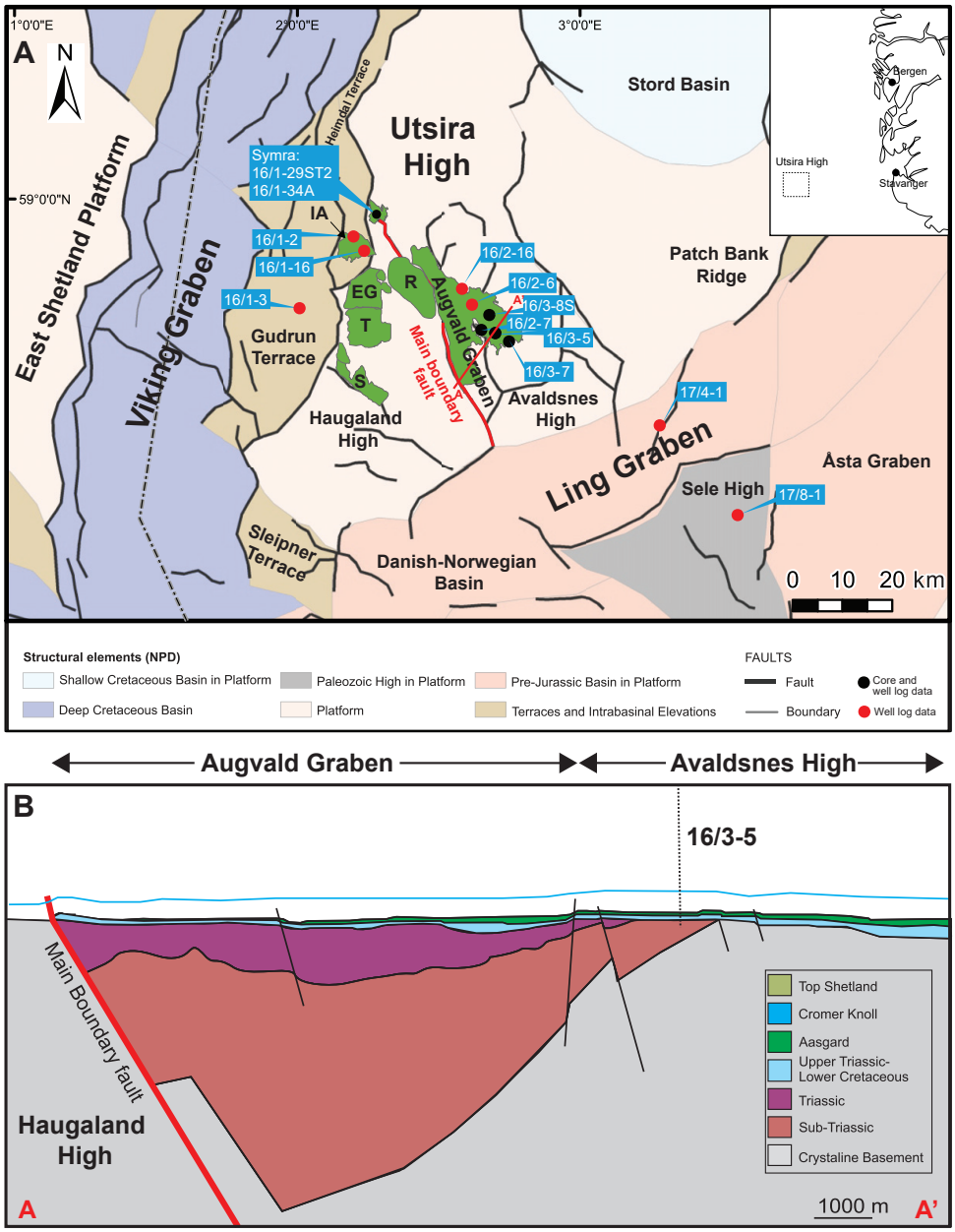

Fig. 1. (A) Simplified map of the greater Utsira High area showing names mentioned in the text, the locations of the investigated wells, and the main faults. The green areas outline oil- and gasfields and prospects including the giant Johan Sverdrup oilfield. Abbreviations: EG: Edvard Grieg; IA: Ivar Aasen; R: Ragnarock; S: Solveig; T, Troldhaugen. (B) Cross-section along the line A-A' in Fig. 1A. The Zechstein succession is preserved beneath Triassic sediments in the Augvald Graben and beneath Jurassic sediments on the Alvaldsnes High. Modified from Ottesen *et al.* (2022).

represent the local erosional remnants of a thicker and laterally more widespread platform succession which is unconformably overlain by sediments ranging in age from Early Triassic to early Paleocene (Danian). Ottesen *et al.* (2022) recently outlined the Mesozoic geology of the Johan Sverdrup field with a focus on the main reservoir intervals. Building on that paper, the present contribution aims to provide a sequence stratigraphic and sedimentological overview of the underlying Zechstein Supergroup to better constrain the stratigraphic, depositional and diagenetic factors which control the variability of reservoir properties of the Zechstein platform carbonates in this area (cf. Sorento *et al.*, 2018).

The Zechstein deposits on the Utsira High range in thickness from ~25 to 100 m and the succession is too thin to be internally subdivided based on seismic data, Correlations are based on core and wireline log data from 13 wells which penetrate down into the Zechstein (Fig. 1). We interpret the drilled carbonates to belong to the Zechstein ZS2 and ZS3 sequences (c.f. Daniels *et al.*, 2020); or lithostratigraphically to the Upper Ca1 (Z1) and Ca2 (Z2) units (Sorento *et al.*, 2018). The carbonate succession is divided by a thin, <5 m

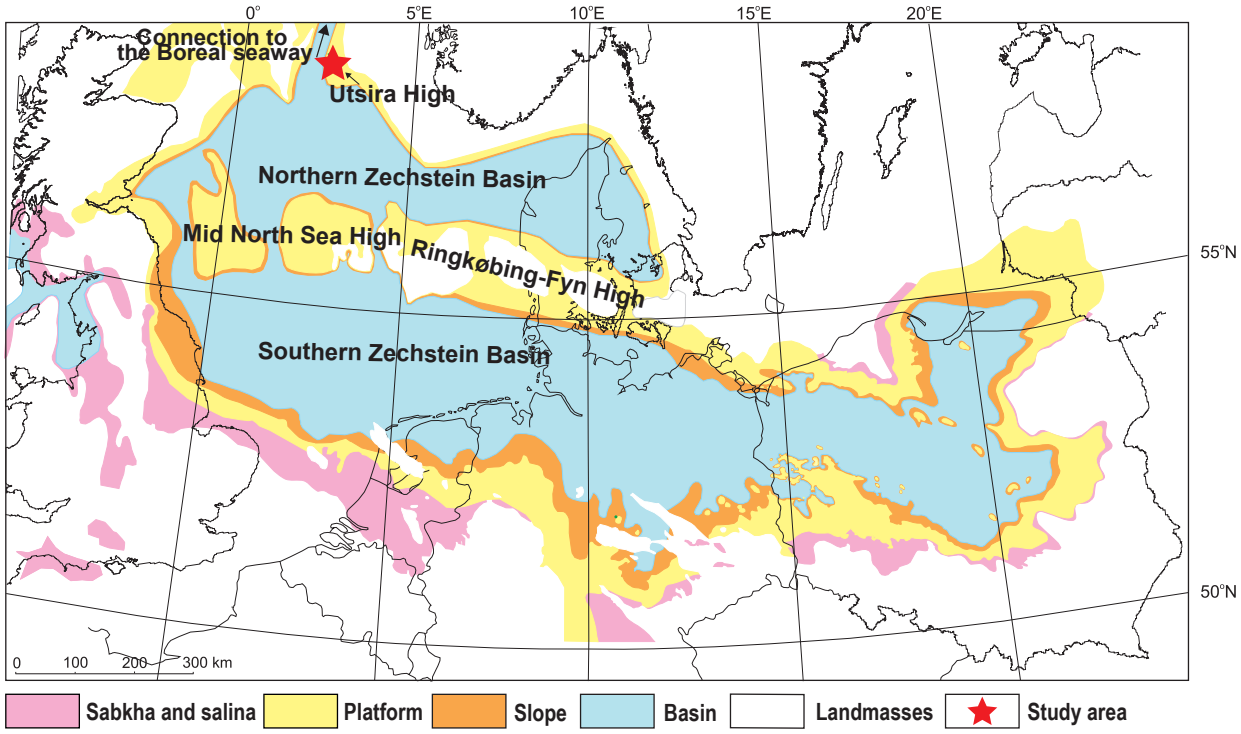

Fig. 2. Generalized palaeogeographic reconstruction of the Zechstein Basin during the ZS3 highstand (= Z2 carbonate, Ca2), showing the distribution of shelf carbonates along the rim of the basin and over the mid North Sea – Ringkøbing-Fyn High. Modified from Słowakiewicz *et al.* (2018).

thick shale-rich TST deposit which is stratigraphically correlated to the ZS3 anhydrite (A1 (Z1)) in sections on the slope (cf. Fyfe and Underhill, 2023 *this issue*). Both the ZS2 and ZS3 carbonates have undergone early diagenetic, pervasive dolomitization and share similarities with Zechstein-aged carbonate reservoir rocks elsewhere in the region (Clark, 1980; Stentoft, 1990; Strohmenger *et al.*, 1996; Sorento *et al.*, 2018). A later phase of dedolomitization and calcitization with a highly negative influence on reservoir quality has been recorded in several wells and constitutes a major exploration risk in the area.

Regional setting

The Utsira High is located in the Norwegian sector of the North Sea to the east of the north-south oriented Viking Graben and the NE-SW oriented Ling Graben (Fig. 1A). During the Late Permian, the High formed part of the northern margin of the NW European Zechstein Basin, close to the connection with the Boreal Ocean (Fig. 2) (Scotese and Langford, 1995; Ziegler, 1990). The Zechstein Basin is divided by the Mid North Sea – Ringkøbing-Fyn High into the larger Southern Zechstein Basin and the smaller, less well-known Northern Zechstein Basin (Fig. 2).

The Utsira High (Fig. 1) is a basement high in which eroded remnants of Permian and Mesozoic rift basin successions are overlain and onlapped by an up to 1500 m thick package of Cenozoic sediments (Serck *et al.*, 2022). The High is separated from the Ling Graben to the south by a NW-SE trending fault system considered to be part of the Sorgenfrei-Tornquist Zone, a long-lasting fault system separating the stable European Platform from the subsiding sedimentary basins to the west and SW (Pegrum, 1984). To the west, the High is separated from the north-south oriented Viking Graben by the Gudrun and Heimdal terraces (Fig. 1).

The Utsira High is divided by the NW-SE striking Main Boundary Fault into the southwestern Haugland High, where basement is covered by a thin Cretaceous succession (Edward Grieg and Ragnarock discoveries); and an eastern, rotated half-graben where Permian and Triassic sediments are locally preserved beneath Upper Jurassic – Danian sediments. The western and deepest part of the Permian – Triassic graben is divided into a number of structural elements and collectively named the Augvald Graben (Ottesen *et al.*, 2022 figure 9). The more proximal and uplifted part of the older half-graben is part of the Avaldsnes High in Fig. 1. The first phase of differential uplift and erosion of the Zechstein succession occurred during a very late Permian and Early Triassic rift phase. Reactivation of the Rotliegend fault system resulted in fault-block rotation and deposition of Triassic strata forming a wedge-shaped geometry dipping towards the Main Boundary Fault.

Later, thermal doming in the mid-Jurassic caused widespread uplift and erosion in the northern North Sea area, and Upper Jurassic sediments rest directly on eroded Zechstein carbonates over wide areas of the

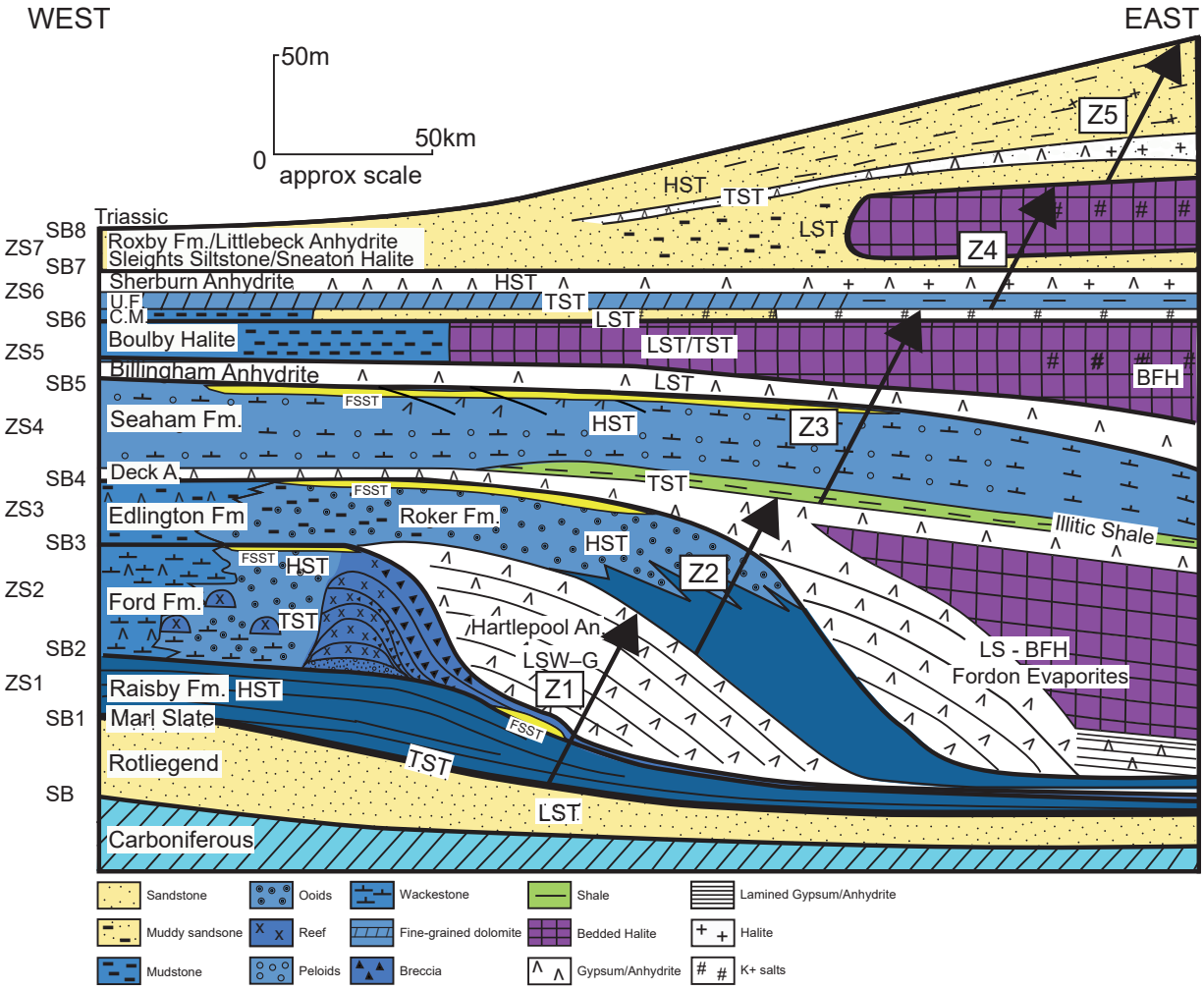

Fig. 3. Comparison of Zechstein sequence stratigraphic (ZS) nomenclature of Tucker (1991) and formation names in NE England with lithostratigraphic Zechstein cycles (Z1-) after Richter-Bernburg (1955). Modified from Tucker (1991) and Daniels *et al.* (2020).

Avaldsnes High, including wells 16/3-5 and 16/3-7 (see Fig. 1). Late Jurassic – Early Cretaceous rifting and crustal-scale rollover led to re-exposure of the Utsira High (Thomas and Coward, 1996; Riber *et al.*, 2015; Serck *et al.*, 2022). From the Cretaceous, the area was characterized by tectonic quiescence and regional thermal subsidence resulting in the deposition of a 1500 m thick post-Jurassic sequence (Riber *et al.*, 2015; Sorento *et al.*, 2018; Serck *et al.*, 2022).

The depositional evolution of the Southern Zechstein Basin is well documented based on studies of outcrop, well and seismic data, summarized in Tucker (1991), Kiersnowski *et al.* (1995), Taylor (1998), Peryt *et al.* (2010),Grant *et al.* (2019) and Fyfe and Underhill (2023, *this issue*). The carbonate-evaporite dominated succession is conventionally divided into 5–7 carbonate-anhydrite-halite cycles (Z1 to Z5/Z7) (e.g. Richter-Bernburg, 1955; Stemmerik and Frykman, 1989; Fyfe and Underhill, 2023 *this issue*), or 7–8 depositional sequences (ZS1-ZS7/ZS8: Tucker, 1991) reflecting flooding of the basin followed by restriction and evaporation (Fig. 3). Carbonates are confined to the lower part of the succession (Z1-Z3 – ZS1-ZS4) and are most thickly developed along the basin margins whereas the basin centres are dominated by thick halite deposits (Taylor, 1998; Grant *et al.*, 2019).

The depositional evolution of the Northern Zechstein Basin is less well-known. Based on 2D seismic data and well information, Clark *et al.* (1998) mapped four depositional zones (DZ1-4) in the UK sector; more recently, Jackson *et al.* (2019) extended this work to cover most of the Norwegian part of the basin. The depositional zones (DZs) reflect the approximate percentage of halite in the section: DZ1 (<10% halite) occurs along the basin margins, DZ2 (10-50% halite) and DZ3 (50-80% halite) occur on basin-dipping ramps, and DZ4 (>80% halite) occurs in basin centre locations (Clark *et al.*, 1998; Jackson *et al.*, 2019). From Fig. 2 it is evident that the halite-dominated DZ2-4 zones cover most of the Northern Zechstein Basin. The less than 100 m thick, carbonate-dominated Zechstein succession on the Utsira High belongs to DZ1 and was deposited on a tectonically more stable block.

The Zechstein succession is thickest and stratigraphically complete in the Viking and Ling grabens where the halite-dominated successions representing DZ4 are >1000 m thick. The thickest and most complete DZ1 successions occur beneath Triassic shales in wells 16/2-6, 16/2-7 and 16/2-16 east of the Main Boundary Fault (Figs 1, 4), and on the Gudrun Terrace and the intrabasinal Sele High (Figs 1, 4, 5). Thinner and stratigraphically less complete successions have been drilled on the SE part of the Avaldsnes High and towards the north.

DATASET AND METHODS

This study integrates core and wireline log data from 13 wells in the greater Utsira High area (Fig. 1A). Slabbed cores are available from six exploration wells: 16/2-7 in the Augvald Graben; 16/3-5, 16/3-7 and 16/3-8S on the Avaldsnes High; and 16/1-29ST2 and 16-1/34A at the Symra field (Figs 1, 4-6). The main focus is on wells drilled over the last decade since they allow the integration of a wide range of petrophysical logs – including gamma-ray, bulk density (RHOB), resistivity, neutron porosity (NPHI), sonic and photoelectric logs – with core material. To identify lithologies in the Zechstein Supergroup, observations from the wireline logs were combined with core and cuttings data from all the investigated wells. The core and cuttings data were tied to their petrophysical well log response and extrapolated to identify the principal lithologies in non-cored wells.

The extensive coring of the Zechstein carbonates has helped to establish a firm distinction between dolomite and calcitized lithologies; this is important because the calcitized carbonate intervals are completely recrystallized and without porosity. The two lithologies are best distinguished using resistivity and photoelectric values integrated with the combined response from NPHI and RHOB logs (see Fig. 6). Cored calcitized intervals are characterized by significant variability in deep resistivity values ranging from 2.8 to 260.7 ohm.m (n = 353). This is much higher than the resistivity values from the dolomitized intervals, which are in the range 0.7–14.3 ohm.m (n = 264). Also, the photoelectric values are higher in the calcitized intervals, ranging from 3.1 to 6.4 B/E, with an average of 5.0 ±0.6 B/E (n = 261), compared to 2.7 – 7.0 B/E (average 3.9±0.7: n = 353) for the dolomite. Anhydrite intervals are distinguished from calcite and dolomite lithologies by the distinct positive separation of their NPHI/RHOB values, which are characterized by high RHOB values at 2.98 g/cm^3 and low NPHI values at 0.00 v/v (Rider and Kennedy, 2011).

To constrain the timing of the calcification event, U/Pb dating of the main diagenetic phases from the calcitized carbonate intervals in wells 16/3-8S and 16/3-5 was carried out. Polished thin sections with a thickness of 100 μm were prepared for each sample and were characterized using a petrographic microscope followed by μXRF (X-ray fluorescence) element mapping at the Norwegian University of Science and Technology (NTNU), Trondheim, to identify different generations of carbonate minerals. Selected areas in these thin sections were screened using a laser ablation (LA) system with an inductively coupled plasma mass spectrometer (ICP-MS) at the University of Tartu (Estonia) to determine the U and Pb content, as well as the abundance of elements indicative of silicate mineral contamination (e.g. Al, Th, Ti). Areas containing elevated U contents from screened samples (each approximately several mm^2) potentially suitable for U-Pb dating were then mapped in high resolution using LA ICP MS. Guided by the LA ICP MS mapping results, selected samples were dated using an LA system coupled to a multi collector ICP MS at the Natural Environment Research Council Isotope Geosciences Laboratory (Nottingham, UK) following Roberts *et al.* (2017). Laser spot sizes of 45 and 80 μm were used depending on the size of the target, and WC-1, Duff Brown and NIST 614 were used as SRMs (Hill, 2016; Roberts, 2017). LA ICP MS mapping data and U-Pb geochronological data were reduced using the Iolite 4 software package (Paton *et al.*, 2011; Petrus *et al.*, 2017), with final ages and Tera-Wasserburg diagrams created using IsoplotR (Vermeesch, 2018). All ages are reported with 2σ uncertainties.

Ages from the four samples presented here span a range from 225.0 ± 61.1 Ma to 151.7 ± 88.3 Ma. The MSWDs (mean squared weighted deviations) of these samples are reasonably good, ranging from 1.2 to 2.7, but the resulting age uncertainties are extremely large because of the low U contents within the samples. Two samples from depths of 2004.74 m (225.0 ± 61.1 Ma) and 2010.60 m (216.2 ± 66.2 Ma) from well 16/3-8S yield a combined age of 218.1 ± 62.2 Ma for calcitization (i.e. dedolomitization), whereas recrystallized calcite from depths of 2010.60 m in well 16/3-8S and 1934.25 m in well 16/3-5 yield ages of 162.7 ± 76.0 Ma and 151.7 ± 88.3 Ma, respectively.

STRATIGRAPHY OF THE ZECHSTEIN GROUP

We have identified seven main lithologies in the Zechstein Group in the study area based on the integration of wireline petrophysical logs with core and cuttings data: (i) dolomite; (ii) calcitized carbonates; (iii) anhydrite; (iv) halite; (v) K-salt; (vi) marly limestones, and (vii) shales (Fig. 4). Regional stratigraphic correlation was based on the identification of key surfaces in the logs, and sequences

were annotated using the nomenclature of Tucker (1991) (Fig. 3). The succession shows pronounced variations in lithology and thickness comparable to those described from studies in the Southern Zechstein Basin (e.g. Tucker, 1991; Grant *et al.*, 2019; Fyfe and Underhill, 2023 *this issue*), and for simplicity three broad environments of deposition were differentiated – shelf, slope and basin – within a conceptualized shelf-to-basin transect (Figs 4, 5).

Key surfaces

The Upper Permian Zechstein rests unconformably on older Permian Rotliegend sediments in all wells except well 16/1-34A, where it rests on basement. The sequence boundary separating the basal Zechstein (ZS1) Kupferschiefer/Marl Slate from the underlying Rotliegend succession (SB1) was not cored in any of the wells and the precise nature of the transition is not known.

SB2 divides the ZS1 succession from the overlying ZS2, but this sequence boundary is difficult to identify in the study area. SB1 is overlain by marly limestones up to ~50 m thick in wells drilled in slope and basinal settings on the Utsira High (wells 16/1-3, 17/8-1 and 17/4-1), and by a thinner, mostly ~2-3 m thick shale unit in shelf areas (Fig. 4). These shales are regarded as belonging to ZS1 and ZS2 and accordingly are partly equivalent to the Kupferschiefer – Marl Slate in basinal and slope settings. This is based on identification of SB3 at the base of the Hartlepool-Werra anhydrite equivalent immediately above the shale unit in well 17/8-1 (Fig. 4). The high gamma-ray unit at the base of the Zechstein succession across the Utsira High is suggested to be composed of transgressive deposits at the base of ZS2, and accordingly the boundary at the base of the Zechstein Group is a combined SB1 and SB2.

In platform areas, the carbonate succession is divided into two by a distinctive gamma peak in wells 16/1-2, 16/1-16, 16/2-7, 16/2-16, 16/3-8S and 16/3-5. The base of the gamma excursion is identified as the sequence boundary (SB3) between ZS2 and ZS3 in accordance with the stratigraphic subdivision established by Sorento *et al.* (2018), and forms the foundation for the stratigraphic scheme presented here (Fig. 4). The SB3 is identified as a distinctive shift from carbonates and marly limestones to anhydrite in wells 17/8-1 and 16/1-3 located on adjacent terraces and intrabasinal highs and condensed marly limestones in well 17/4-1 in the Ling Graben. Well log data from the Utsira High have not enabled us to further subdivide the oldest carbonate unit, so it is possible that the succession beneath SB3 also includes sediments belonging to ZS1.

The top of ZS3 is an erosional unconformity across most of the Utsira High, with the exception of wells 16/2-6, 16/2-7 and 16/2-16 located in the deeper parts of the Permian-Triassic graben to the east of the Main Boundary Fault (Figs 1, 4). In these wells, and well 16/1-3 on the Gudrun Terrace, SB4 is identified by an abrupt increase in gamma values and a shift towards the deposition of marly limestones. In wells 17/8-1 and 17/4-1, the boundary is defined by a shift from carbonates to anhydrite.

The top of ZS4 is recognized as an abrupt shift from marly sediments to anhydrite in wells 16/2-7, 17/8-1 and 17/4-1 (Fig. 4). It is an erosional unconformity overlain by Triassic sediments in wells 16/1-3, 16/2-6 and 16/2-16. Zechstein sediments younger than the basal ZS5 (Billingham) anhydrite are only preserved in basinal areas (well 17/4-1) belonging to the DZ 2-4 zones of Jackson *et al.* (2019).

Sequence ZS1

We propose that sequence ZS1 is restricted to slope and basinal areas. However, it is unclear how far updip the initial Zechstein transgression reached. Deposition is dominated by fine-grained siliciclastics. The combined thickness of ZS1 and ZS2 is less than 5 m on the Sele High (well 17/8-1) and even thinner in the centre of the Ling Graben (well 17/4-1; Figs 4, 5). It is thicker along the eastern margin of the Viking Graben where it forms a 10-50 m thick wedge on the Gudrun Terrace.

Sequence ZS2

Sequence ZS2 is carbonate dominated and forms an up to 40 m thick carbonate shelf succession overlying a thin transgressive mudstone unit on the Utsira High. The carbonates thicken to 60 m in the more distal well 16/1-3 before disappearing or becoming very thin in the basins where ZS2 is condensed (Fig. 4). Based on macro- and microfacies analysis of cored material in wells 16/2-7, 16/3-5, 16/3-7 and 16/3-8S, Sorento *et al.* (2018) identified 11 facies which all reflect deposition in shallow shelf and arid shoreline environments with a regular input of terrestrial material such as silty quartz and mica grains. The facies are organized in three facies associations, and their distribution suggests a segmentation of the shelf into an eastern shallow platform dominated by peritidal deposits and a western shallow intra-shelf basin dominated by muddy facies in the Augvald Graben (Sorento *et al.*, 2018).

Generally similar shallow-shelf environments are recognized from the Symra area where seven carbonate facies have been identified in cored material from wells 16/29ST2 and 16/1-34A (Blinkenberg *et al.*, *in prep.*). In this area, the ZS2 carbonates form an overall shallowing-up succession of outer-ramp mudstones and mid-ramp tempestites rich in detrital grains, passing upward into inner-ramp microbialites and capped by oolitic high-energy shoals and beach deposits (Blinkenberg *et al.*, *ibid.*).

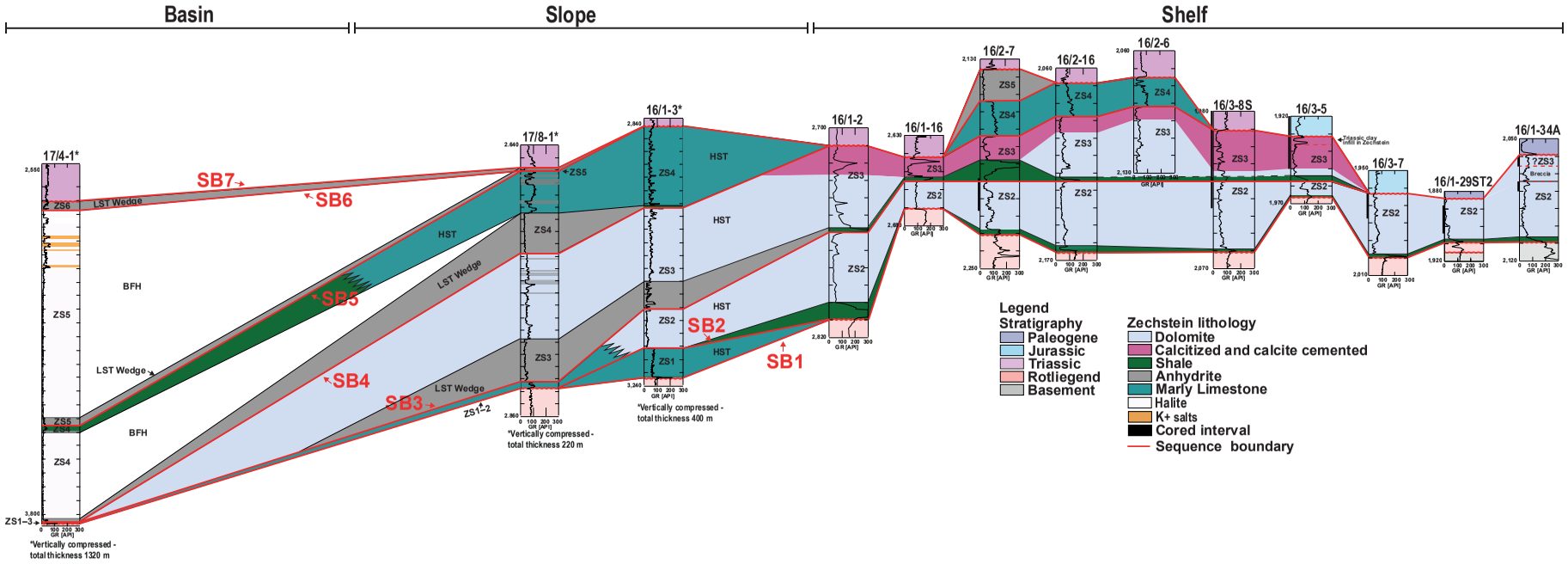

Fig. 4. Well log panel showing the gamma-ray log response of selected wells on the Utsira High and adjacent terraces and basins. The main lithologies are identified based on responses from the full suite of logs. Note different vertical scales on the logs from the three wells drilled in the basin and on the slope. Stratigraphic nomenclature and sequence boundaries according to Tucker (1991); see Fig. 3. For location of wells, see Fig. 1. Note that the panel is organized to illustrate the extent of the calcitized interval on the shelf and an idealized shelf-to-basin transition.

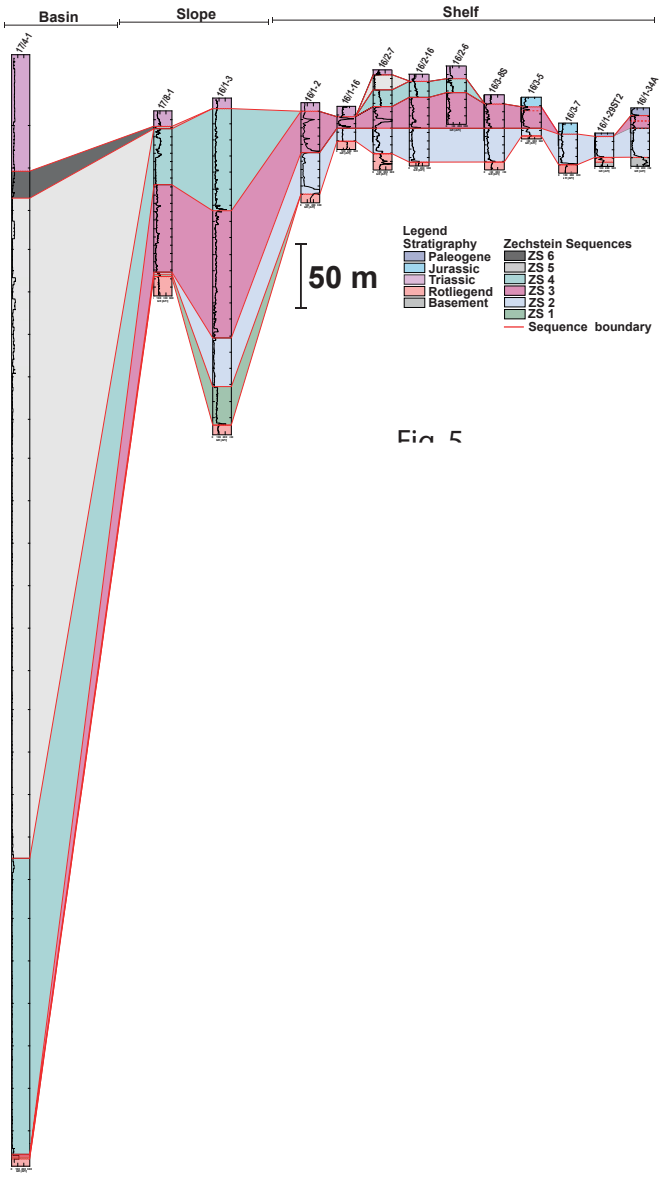

Fig. 5. Thickness variations of sequences ZS1-ZS6. Note the outbuilding of sequences ZS3-ZS5 towards the basin centre. Also note the huge differences in thickness from the Utsira High to the adjacent basins and the preservation of the shelf-to-basin relief until the accumulation of halite during ZS5 time.

Sequence ZS3

In slope areas, massive anhydrite units up to 60 m thick, equivalent to the Hartlepool and Werra anhydrites, onlap SB3 and form a lowstand wedge basinward of the ZS2 carbonate shelf edge. The anhydrite passes landwards into a thin interval of carbonates and siliciclastics characterized by slightly higher gamma values. This interval is only cored in well 16/3-8S where it is made up of 5 m of algal laminated carbonate bindstones which are interpreted as sabkha deposits (Sorento *et al.,* 2018). Across the Utsira High, ZS3 is carbonate dominated and up to 50 m thick in stratigraphically complete sections. It is thinner or locally missing in many wells due to post-Permian erosion (Fig. 4). The carbonate unit thickens to 70-120 m where it overlies the ZS3 anhydrite unit in slope settings before thinning and disappearing in the basins.

The ZS3 shelf carbonates have been cored in wells 16/3-5, 16/3-8S and 16/1-34A. In the 16/3-5 and 16/3-8S cores, most of the original depositional fabric has been destroyed by dedolomitization and fabrics resembling oolitic grainstones, microbialites and various mudstones have only rarely been identified (Sorento *et al.*, 2018). In well 16/1-34A, cored material possibly belonging to the ZS3 sequence consists of dolomitized carbonate grainstones rich in silt-sized quartz and K-feldspar grains. Deposition is interpreted to have occurred in marginal marine environments. In well 16/1-34A, the transition between the ZS2 and ZS3 appears to be overprinted by later faulting which resulted in brecciation of the carbonates. This interval is not fully cored, and the precise nature of this important boundary is still uncertain.

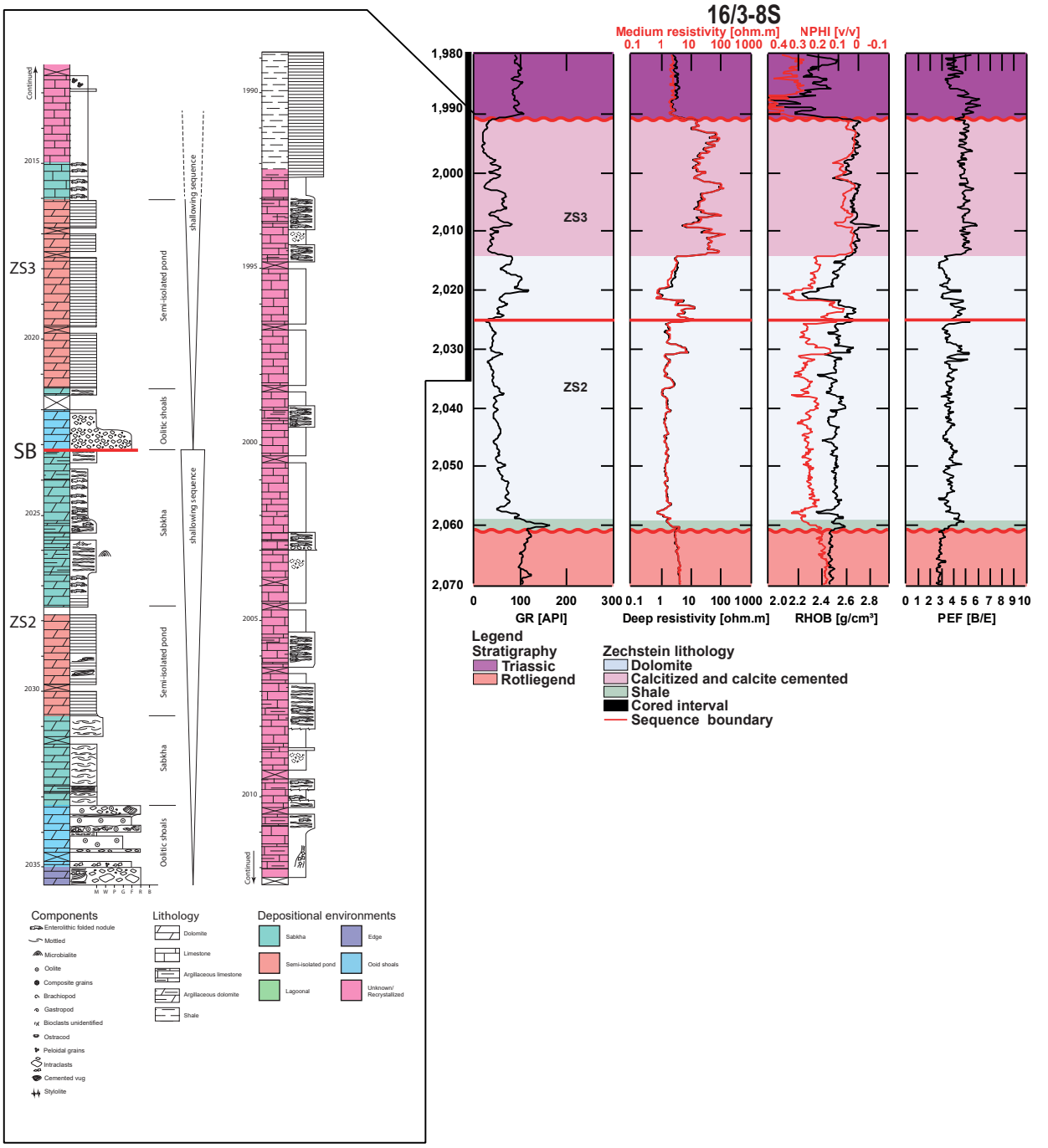

Fig. 6. Sedimentological log of the cored Zechstein interval in well 16/3-8S (modified from Sorento *et al.*, 2018) and corresponding well log panel to illustrate the shift in log response from dolomite to calcitized carbonate. The calcitized intervals are characterized by higher resistivity and photoelectric (PEF) values and smaller separation between density (RHOB) and porosity (NPHI) values. Note that the calcitized intervals are not distinguishable in the gamma-ray log (GR).

Sequence ZS4

Sequence ZS4 is preserved as a 15-20 m thick siltstone and marl unit resting directly on calcitized ZS3 carbonates in wells 16/2-6, 16/2-7 and 16/2-18 in the Permian-Triassic half-graben east of the Main Boundary Fault. The transition has not been cored. In slope settings, 40-120 m thick marly units overlie 5-30 m thick anhydrite units corresponding to the Fordon-Basal Anhydrite (Fig. 4); and in basinal successions, the marlstones overlie thick (+300 m) halite corresponding to the Stassfurt Halite (Figs 4, 5).

Sequence ZS5-ZS6

Sequence ZS5 is composed of 20 m of massive anhydrite in well 16/2-7 that thickens to 25 m in well 17/4-1 in the Ling Graben (Fig. 4). Less than 2 m of

anhydrite is preserved in the same stratigraphic position in well 17/8-1, and the anhydrite unit is regarded as equivalent to the Billingham Anhydrite of onshore NE England. In the Ling Graben, the anhydrite is overlain by thick (? 800 m) halite with thinner layers of carnallite in the upper part. This unit corresponds to the Boulby and Leine Halites and is overlain by 30 m of anhydrite belonging to ZS6 in well 17/4-1.

CARBONATE RESERVOIR DESCRIPTION

The giant Johan Sverdrup oil field on the Utsira High has estimated reserves in the order of 2.2-3.2 billion barrels with most of the oil in-place contained in the Upper Jurassic – Lower Cretaceous Viking Group and only a negligible fraction in the Zechstein carbonates (Ottesen *et al.*, 2022). Conversely, the ZS2 and ZS3 carbonates form a significant component of the reservoir in the Symra discovery where much of the oil in-place is contained in weathered basement rocks. In the following paragraphs, the diagenesis, reservoir potential and lateral variability of the Zechstein carbonates are described and evaluated within the sequence stratigraphy framework outlined above.

Reservoir potential of the ZS2 shelf carbonates

The ZS2 carbonate shelf deposits attain a maximum thickness of 40 m on the Utsira High and overall are characterized by fair to good reservoir properties (10-35% porosity, and permeability of up to 10,000 mD). ZS2 carbonates are preserved in all wells reaching the base Zechstein, and they are likely to be widely distributed in the area to the east of the Main Boundary Fault. The ZS2 carbonates are pervasively dolomitized, and from a reservoir perspective they can be divided into two groups:

(i) in the first group are carbonates replaced by an early, texture-preserving dolomite (cf. Sorento *et al.*, 2018), which are particularly common in wells 16/2-7 and 16/3-8S and which are characterized by fair reservoir properties (Fig. 7);

(ii) later modification of the fabric in the form of recrystallization and precipitation of mainly non-planar crystals, up to 50 µm in size, resulted in dolomites with improved reservoir properties both in terms of increased permeability and overall higher porosity. This fabric dominates in the 16/1-29ST2 and 16/1-34A wells from the Symra discovery and in well 16/3-7 (Fig. 7). Stable isotope data in Sorento *et al.* (2018) show that the dolomites in 16/3-7 are characterized by more negative $\delta^{18}O$ values than dolomites in 16/3-8S and 16/2-7 (Fig. 8).

Reservoir potential of ZS3 shelf carbonates

The ZS3 carbonate shelf deposits are 30-50 m thick in most wells drilled on the Utsira High (Figs 4, 5). Thinner ZS3 intervals in wells 16/1-16 and 16/1-34A are likely to be the result of later erosion, and ZS3 carbonates are missing entirely in wells 16/1-29ST2 and 16/3-7 (Fig. 4). The ZS3 shelf carbonates are divided into two units based on distinctive differences in the diagenetic fabrics.

The ZS3 carbonates are preserved as dolomite in slope sections outside the Utsira High and in the lowermost part of the ZS3 carbonate interval in many of the wells drilled on the platform (Fig. 4). The interval preserved as dolomite is thin (0-10 m) and discontinuous over large areas of the Utsira High, and thicker ZS3 dolomite intervals (25-35 m) have only been drilled in wells 16/1-2, 16/2-6 and 16/2-16 (Fig. 4). Core material of ZS3 dolomite is only available from wells 16/1-34A and 16/3-8S. The dolomites in well 16/3-8S have porosities of 1.2 to 35.3%. Stable isotope data from well 16/3-8S show a large spread in $\delta^{18}O$ values (Fig. 8; Sorento *et al.*, 2018).

The upper part of ZS3 is calcitized and calcite-cemented over a large area. The calcitized interval has been identified in well logs across the Utsira High and forms a regional, laterally widespread unit that appears to thin from 20-25 m in the SE to 10-15 m in the (N-)W (Fig. 4). Dedolomite is not present in well 16/1-34A where just the basal few metres of ZS3 are preserved, and is missing in wells drilled in slope and basinal positions (Fig. 3). The calcitized unit has been drilled in wells 16/3-5 and 16/3-8S, where it is characterized by poor reservoir properties (porosities mostly <5% and permeabilties <0.1 mD; Fig. 7) (Sorento *et al.*, 2018). Stable isotope data from calcitized phases in wells 16/3-5 and 16/3-8S show that $\delta^{18}O$-values fall in a narrow range between -5 and -8 ‰ whereas the $\delta^{13}C$-values shows a larger spread from +3 to -6 ‰ (Fig. 8). Calcitized carbonates from well 16/3-8S are overall characterized by more positive $\delta^{13}C$ values.

In wells 16/3-5 and 16/3-8S, red and green calcareous clay fills voids, cracks and breccias in the upper part of the dedolomitized unit, and the presence of the Triassic palynomorph *Porcellispora longdonensis* within the clay in the former well was used to infer a latest Permian to earliest Triassic age for the subaerial exposure and dedolomitization event (Sorento *et al.*, 2018). However, in order to better understand the lateral extent of the dedolomitized unit and its sequence stratigraphic position at the top of the ZS3, the timing of the calcite replacement was further investigated by dating calcite crystals from wells 16/3-5 and 16/3-8S utilizing U/Pb geochronology. The results are given in Fig. 9. Data from well 16/3-8S indicate a first phase of dedolomitization in the Triassic (218.1 ± 62.2 Ma) followed by a later phase in the Middle to Late Jurassic (162.7 ± 76 Ma); whereas the dedolomite in 16/3-5 gives a slightly younger Late Jurassic age (151.7 ± 88 Ma).

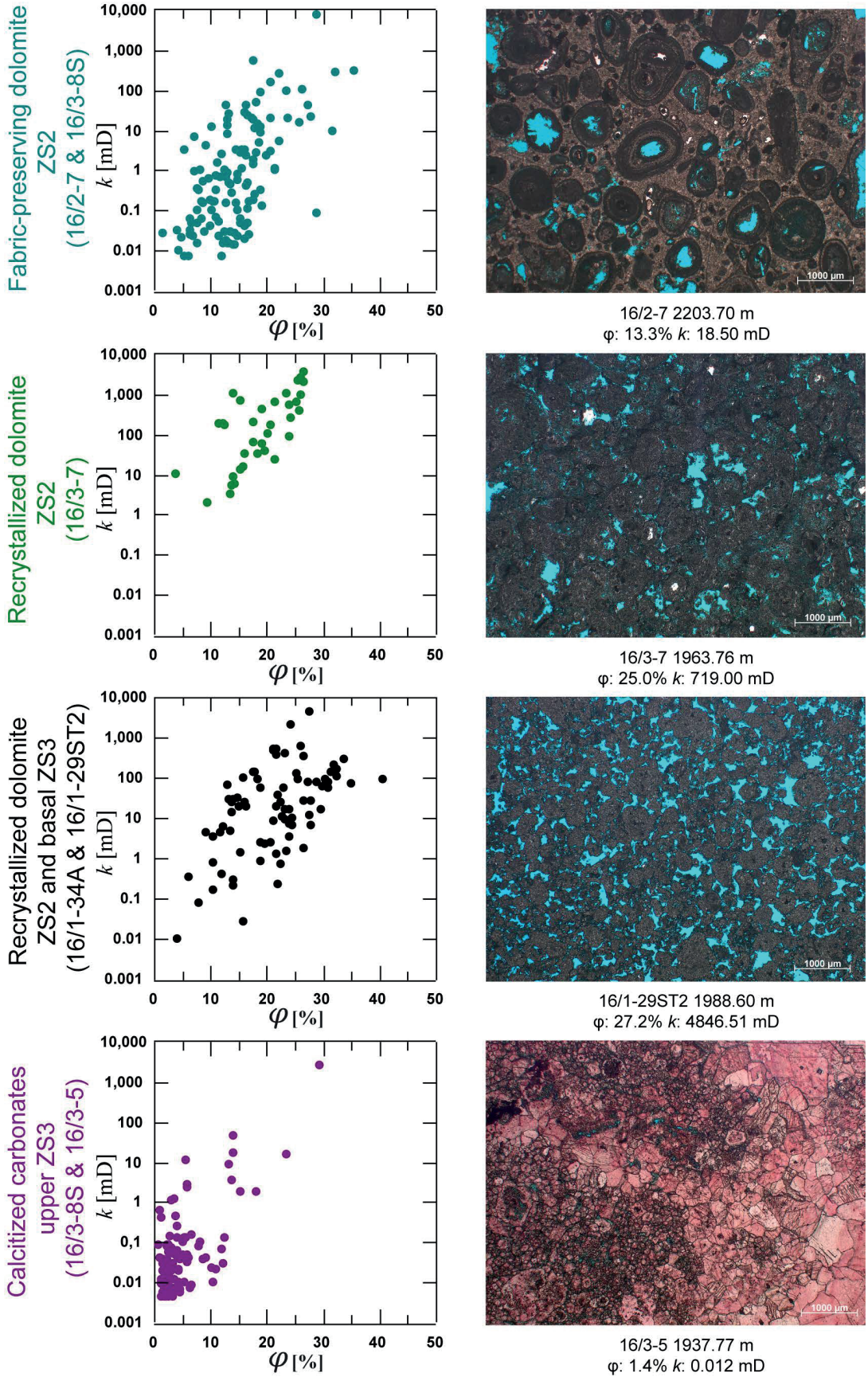

Fig. 7. Photomicrographs of the main carbonate fabrics and the porosity and permeability characteristics from core plug measurements. The first, fabric-preserving phase of dolomitization resulted in fair reservoir properties whereas later recrystallization greatly improved both porosity and permeability. Calcitization resulted in a reduction in both porosity and permeability.

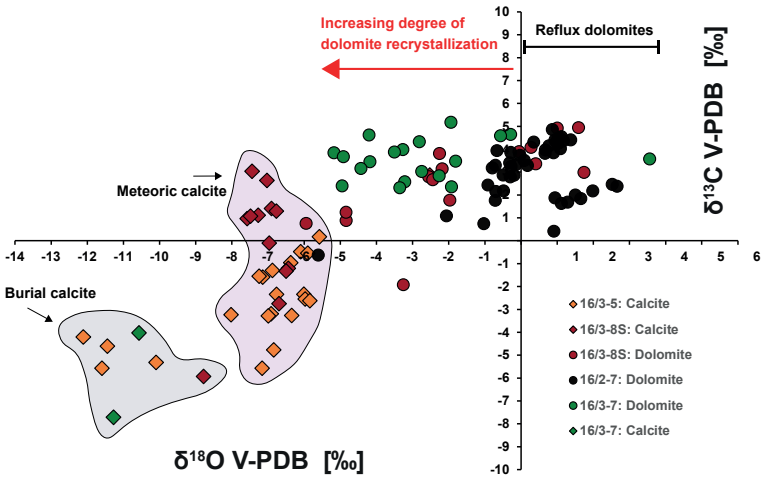

Fig. 8. Stable isotope data of Zechstein carbonates from the Utsira High. Modified from Sorento *et al.* (2018). Note the shift towards negative oxygen isotope values during recrystallization of the dolomite, and the two populations of oxygen isotope values of the calcite formed during meteoric diagenesis.

DISCUSSION

The first detailed description of the Zechstein carbonates drilled on the Utsira High was given by Sorento *et al.* (2018). In the present contribution, we have focused on providing a more robust stratigraphic framework for the Zechstein succession based on a re-interpretation of well log data, with a particular focus on delineating the extent of dedolomitized strata across the greater Utsira High. Based on the distinct well log response of the dedolomite, calcification appears to be stratigraphically restricted to the upper part of ZS3 and thus forms a useful marker across the Utsira High (Fig. 4). The sequence stratigraphic scheme forms the basis for comparison with the Southern Zechstein Basin, the adjacent Shetland Platform and the Upper Permian succession in East Greenland. The carbonate facies and the overall stratigraphy encountered on the Utsira High are broadly similar to that recognized in the Southern Zechstein Basin (e.g. Stemmerik and Frykman, 1989), whereas the diagenesis of the ZS2 and ZS3 shelf carbonates indicates pervasive fresh-water infiltration and recrystallization similar to that which has been described from Permian carbonates in East Greenland (Scholle *et al.*, 1991, 1993). However, the timing of these processes seems to be different on the Utsira High, as discussed below.

Comparison to the Southern Zechstein Basin stratigraphy

The overall stratigraphic development of the greater Utsira High area in the NE corner of the Northern Zechstein Basin as described above is similar to that described from the Southern Zechstein Basin (Stemmerik and Frykman, 1989; Tucker, 1991; Strohmenger *et al.*, 1996; Peryt *et al.*, 2010), at least until ZS6 times. This similarity includes the presence of lowstand anhydrite wedges along the ZS2 and ZS3 carbonate platform margins and ZS4 and ZS5 halite deposits in basin centres (Figs 4, 5). Although the Utsira High data-set is evidently much less comprehensive than that generated from the Southern Zechstein Basin over the last century (see Peryt *et al.*, 2010), some important differences are evident and include:

- the absence of anhydrite at the base of ZS4 in shelf areas (equivalent to the Deck anhydrite);
- the dominance of marly limestones in the ZS4 highstand deposits;
- maximum halite accumulation during ZS5 time rather than ZS4 time; and from a petroleum geological perspective
- widespread dedolomitization of the upper part of the ZS3 shelf carbonates (Fig. 4).

It is also important to note that the drilled ZS2 and ZS3 carbonates on the Utsira High represent deposition in the inner parts of wide carbonate shelves, and that there is so far no evidence of platform margin facies like the bryozoan reefs in the ZS2 Fordon Evaporite Formation in NE England (Smith, 1981; Tucker, 1991) or the extensive oolite shoals belts along the ZS3 platform margin (e.g. Clark, 1980; Clark, 1986).

The absence of anhydrite at the base of ZS4 is considered to be primary, i.e. the equivalent of the Deck Anhydrite was not deposited on the Utsira High. However, given the regionally extensive dedolimitization of the ZS3 carbonates immediately below, it is possible that any overlying anhydrite was dissolved away and contributed as a Ca-source for calcite precipitation (*see below)*. However, in that case, disturbance of the immediately overlying units should be expected, so the lack of a basal ZS4 anhydrite across Utsira High is regarded as a primary feature.

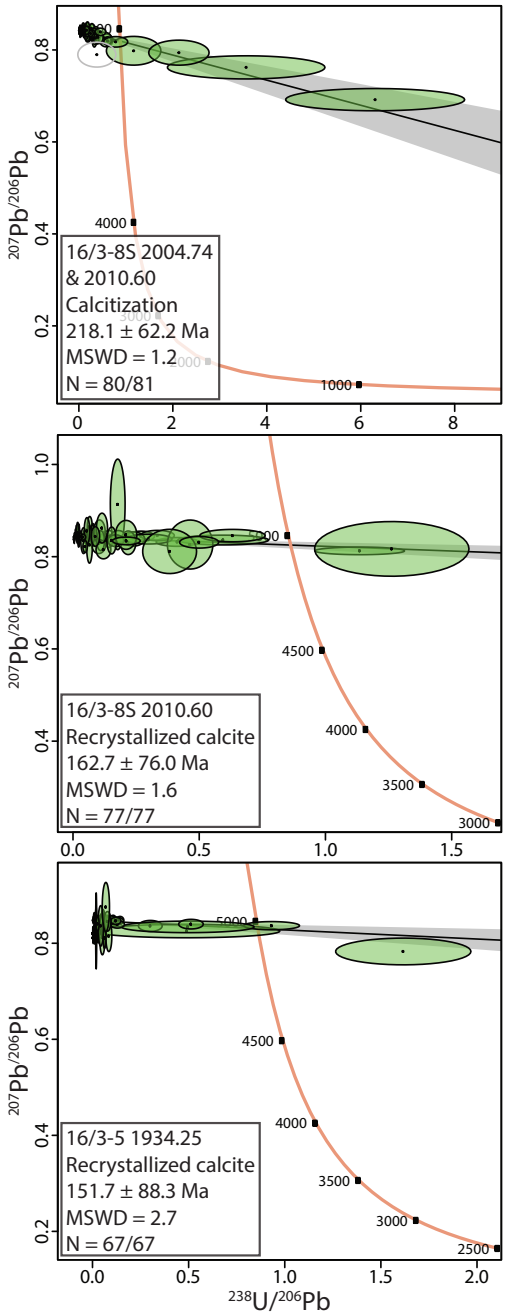

Fig. 9. Tera-Wasserburg concordia plots for the analyzed carbonates. A combined age of 218.1 ± 62.2 Ma (±2σ) from samples from 2004.74 and 2010.60 m in well 16/3-8S provides a date for calcitization. Analyses of recrystallized calcite from wells 16/3-8S and 16/3-5 (depths 2010.60 and 1934.25 m, respectively) yield ages of 162.7 ± 76.0 and 151.7 ± 88.3 Ma, with very large uncertainties due to low amounts of radiogenic Pb. While these ages broadly support recrystallization after the initial calcitization event, and could coincide with a mid-late Jurassic uplift event, the very large uncertainties allow for recrystallization at ca. 220 to 70 Ma and should not be used for detailed interpretation.

The dominance of marly carbonates in the ZS4 highstand indicates a supply of fine-grained siliciclastics from adjacent exposed highs. The carbonates included in ZS3 in the Symra area are relatively rich in siliciclastic material, and ample sources of fine-grained siliciclastic were therefore apparently available during ZS3 and ZS4 times.

The ZS4 carbonates and marly limestones overstep the older platform edges but were unable to fill the basin centres, and the Northern Zechstein Basin remained underfilled into ZS5 time when thick, basin-floor halite successions accumulated in both the Viking Graben and the Ling Graben and southwards in the Danish-Norwegian basin (Fig. 5; Glennie *et al.*, 2003; Jackson *et al.*, 2019).

Timing of the ZS3 calcitization event

Dedolomitization is a common diagenetic process in interbedded carbonate-evaporite successions subjected to subaerial exposure and fresh-water circulation.

Dissolution of $CaSO_4$ during the incursion of undersaturated groundwater releases Ca-ions, and the elevated Ca/Mg ratio results in dedolomitzation (e.g. Canarveras *et al.*, 1996; Schoenherr *et al.*, 2018 for an overview). The most likely source for Ca is $CaSO_4$ units within the Zechstein succession. With reference to the generalized sequence stratigraphic model of Tucker (1991), likely candidates are the anhydrites at the base of ZS4 (Deck anhydrite), ZS5 (Billingham Anhydrite Formation) and ZS6 (Sherburn (Anhydrite) Formation), since the lower Hartlepool and Fordon equivalents are restricted to slope and basin settings around the Utsira High (Fig. 4).

The calcitized top of the ZS3 carbonates on the Utsira High is overlain by sediments ranging in age from Late Permian (Zechstein, ZS4) to Jurassic, with the majority of wells showing Triassic sediments above the ZS3 carbonate (Fig. 4). It is therefore not evident if the dedolomitization is the result of multiple events or formed during one distinctive event. Sorento *et al.* (2018) suggested that calcitization occurred during latest Permian – Early Triassic rifting based on the occurrence of the Triassic palynomorph *Porcellispora longdonensis* in clay-filled caves in the top of the ZS3 calcite. This species has an Anisian-Norian (middle-late Triassic) range according to https://paleobotany.ru/ palynodata/species/13998. This frames the infill of the calcitized and karstified ZS3 carbonate in well 16/3-5 to a ca. 40 Ma time interval between 247 Ma and 208 Ma.

The U/Pb age data from ZS3 calcites are characterized by significant uncertainties due to the low U concentrations, resulting in large uncertainties when determining the precipitation age (i.e. the lower intercept in a Tera-Wasserburg diagram). Data from well 16/3-8S date the first phase of dedolomitization to 218.1 ± 62.2 Ma (Fig. 9). This age is compatible with the palynological data; and combined, these data are taken as evidence for a first phase of dedolomitization during the mid-late Triassic. The presence of larger calcite crystals with a U-Pb age of 162.7± 76.0 Ma suggests localized recrystallization during a younger fresh-water event, as does the U-Pb age of 151.7 ± 88.3 Ma of the calcite in well 16/3-5.

A model with an initial Triassic phase of dedolomitization followed by later fresh-water flushing and partial recrystallization is in line with the stable isotope data, since the "Triassic"-aged calcite in well 16/3-8S is dominated by more positive $\delta^{13}C$ values than the younger calcite in well 16/3-5. Most calcites from well 16/3-8S have $\delta^{13}C$ values in the same range as the dolomite it was replacing (Fig. 8). This suggests that the diagenetic system was rock-buffered during initial replacement. The calcite from well 16/3-5 has $\delta^{13}C$ values outside the range of the original dolomite, and the more negative values suggests that later recrystallization took place in a fluid-dominated system with a source of isotopically light carbon.

The earliest phase of dedolomitization most likely correlates to the poorly-dated Intra-Triassic Unconformity (ITU) in the tectonostratigraphic framework for the Johan Sverdrup field (Ottesen *et al.*, 2022). The ITU is inferred to represent a significant time gap and is marked by changes in structural dip (up to 13°), rejuvenation of faults, and the erosion of up-dip areas (Ottesen *et al.*, 2022). Lithoclasts in the overlying syn-rift deposits include Zechstein carbonates and basement rocks, and show that erosion involved Zechstein sediments, at least locally. It is envisaged that the Ca-enriched fluid percolated down-dip in the highly permeable ZS3 dolomites and reached areas where the ZS3 was buried beneath younger Zechstein ZS4 and ZS5 deposits and lowermost Triassic sediments, as observed in wells 16/2-6, 16/2-7 and 16/2-16.

The later phase of fresh-water infiltration and recrystallization of calcite most likely occurred during mid-Jurassic uplift and prior to the regional, Kimmeridgian-aged flooding surface at the base of the Viking Group (Draupne Formation) (FS 3 in Ottesen *et al.*, 2022). This age assignment is compatible with the U-Pb age of the recrystallized calcite in wells 16/3-8S and 16/3-5 with ages of 162.7± 76.0 Ma and 151.7 ± 88.3 Ma, respectively. It is important to emphasize that these ages have very large uncertainties and are derived from samples with very low amounts of radiogenic lead in which a few more radiogenic data points would strongly impact the lower-intercept ages. These ages should therefore not be interpreted with a high degree of confidence, and can only be used to point broadly toward a reprecipitation event at ca. 200 – 100 Ma.

Timing of dolomite recrystallization in ZS2

ZS2 dolomites characterized by recrystallization and later modification of the fabric seem to be confined to wells where Zechstein carbonates are directly overlain by Jurassic or younger sediments, in contrast to the dolomites with an early, texture-preserving fabric that are all buried beneath younger Zechstein deposits and fine-grained Triassic sediments (Fig. 4). It is therefore tempting to link the recrystallization to a post-Triassic phase of fresh-water infiltration of the ZS2 dolomite in uplifted areas where the overlying impermeable sediments were removed and tie it to the mid-Jurassic recrystallization of calcite in ZS3. However, since there is no evidence of fluids enriched in light carbon isotopes involved in the dolomite recrystallization, this is unlikely to be the case. The recrystallized dolomites have the same positive δC^{13} values as the early reflux dolomites but show lighter δO^{18} values (0 to -5 per mil v-PDB) (Fig. 8), and the isotopic signature points to a rock-buffered process similar to that responsible for the initial calcitization phase.

Reservoir potential of the Zechstein carbonates

The sequence stratigraphic subdivision presented here is below the limit of seismic resolution in the greater Utsira High area, and the evaluations of lithology and reservoir properties depend on well log and core data as well as comparison with the better-investigated Southern Zechstein Basin carbonate platforms. Where well expressed the top Zechstein reflector most likely represents either the ZS5 anhydrite or calcitized ZS3 carbonate suggesting that carbonates of ZS2 age are present below the top-Zechstein seismic reflector across the region, and that ZS3 carbonates are likely also to be present (see Fig. 4).

The reservoir capacity of the ZS2 and ZS3 carbonates is controlled by meteoric diagenetic overprinting an early dolomitized fabric during the early(?) Triassic and mid-Jurassic, and reservoir sweet spots are controlled by the post-Zechstein structural evolution rather than by primary depositional facies. Ultimately, the reservoir potential on the Utsira High is in the ZS2 carbonates with some additional potential in the dolomitic part of ZS3 in well 16/1-34A as documented in the Symra discovery (Blinkenberg *et al.*, *in prep.*).

The facies reported from the ZS2 carbonate shelf by Sorento *et al.* (2018) are characterized by an abundance of coated grains, microbial components, and a limited faunal diversity, and resemble typical ZS2 marginal-marine facies described from the Southern Zechstein Basin (e.g. Stemmerik and Frykman, 1989; Słowakiewicz *et al.*, 2013). There is no clear evidence from well and seismic data of bryozoan carbonate reefs in the ZS2 carbonates on or around the Utsira High. The best reservoir quality in the ZS2 platform facies is recorded in areas where carbonates are directly overlain by Upper Jurassic and younger sediments, as in wells 16/3-5, 16/1-29ST2 and 16/1-34A, and the original fabric-preserving dolomite has been recrystallized (Fig. 7).

Facies observations of the ZS3 carbonate shelf deposits are scarce, since most of the available core material consists of fabric-destructive calcite. Observations from wells 16/1-29ST2, 16/1-34A and 16/3-8S all point towards deposition in shallow-shelf and marginal-marine environments with abundant ooids and abundant siliciclastic input. There is no evidence of stacked, oolitic shoal deposits or other facies similar to the main reservoir prospects along the ZS3 platform margins in the Southern Zechstein Basin (e.g. Clark, 1980). The regional dedolomitization of the ZS3 carbonates may indicate that they formed the main aquifer during subaerial exposure of the Utsira High and acted as conduits for the transport of Ca-enriched fresh water across the platform. The calcitized interval seems to thin towards the (N)W, in line with uplift being greatest on the Avaldsnes High (Fig. 1). This may indicate that thick ZS3 dolomite sections are more likely to occur (if not eroded) in the NW.

Comparison with Upper Permian successions in adjacent areas

Time-equivalent carbonate platform deposits have been described from the Shetland Platform to the west of the Viking Graben (Fig 1) and from the East Greenland Basin to the north (e.g. Scholle *et al.*, 1991, 1993; Stemmerik, 2001).

The time-equivalent Wegner Halvø Formation in East Greenland is a carbonate shelf succession divided by regional subaerial exposure surfaces into three sequence (Stemmerik, 2001). The succession is broadly similar to the ZS1 to ZS3 carbonate platforms in the Zechstein Basin with shelf-edge oolitic grainstone shoals and bryozoan buildups (Scholle *et al.*, 1991; Stemmerik, 2001). However, the East Greenland succession contains no evaporites and was clearly located in a more humid setting than that in which the Northern Zechstein Basin carbonates were deposited. This influenced the diagenesis, since the East Greenland succession is preserved as calcite and porosity is mainly secondary and is limited to the effects of freshwater dissolution.

The older ?middle Permian Karstryggen Formation in East Greenland may possibly be used as a model to understand diagenetic processes on the Utsira High. Here, uplift led to prolonged subaerial exposure resulting in karstification and widespread $CaSO_4$ dissolution leading to pervasive calcitization of dolomite platforms carbonates, demonstrating many similarities to the diagenetic alterations observed in the Zechstein shelf carbonates on the greater Utsira High.

SUMMARY AND CONCLUSIONS

The preserved Zechstein succession is 25-100 m thick on the Utsira High at the northern margin of the European Zechstein Basin. The sediments are the remnants of a thicker platform succession that can be correlated to the thick, halite-dominated basinal sequences in the adjacent Ling and Viking grabens based on identification of lithologies and key stratigraphic surfaces in petrophysical logs. Due to the restricted thickness of the Zechstein succession on the Utsira High, seismic resolution of the different Zechstein sequences is not possible, and their internal subdivision was based entirely on well log and core data.

Carbonates included in the ZS2 and ZS3 sequences are widespread across the Utsira High. They are separated in well logs by a zone with increased gamma ray response. The ZS2 carbonates are up to 40 m thick and are preserved as dolomite. The ZS3 carbonate unit is 30-50 m thick and is divided into a lower,

relatively thin dolomite and an upper 15-25 m thick calcitized unit. Dedolomitization of the upper ZS3 carbonates is believed to be the result of percolation of fresh-water enriched in Ca-ions from the dissolution of Zechstein-aged $CaSO_4$ during a Triassic phase of rifting recognized as the intra-Triassic Unconformity by Ottesen *et al.* (2022). Later stabilization of the recrystallized calcite may have occurred during uplift in the Jurassic. U-Pb measurements provide ages of 162.7 ± 76.0 Ma and 151.7 ± 88.3 Ma, but these are subject to significant limitations due to the stabilization of very small amounts of radiogenic lead and a very small number of radiogenic data points. The reservoir capacity of the shelf carbonates is controlled by meteoric overprinting of an early diagenetic dolomite fabric during the Mesozoic. The calcite replacement of the upper part of the ZS3 carbonate unit reduced porosity to 0-5% during calcitization events dated to the early-mid Triassic and mid-Jurassic. Recrystallization of early fabric-preserving dolomite by percolation of fresh water occurred during an un-dated Mesozoic uplift event. The recrystallization has locally enhanced porosity and permeability, and these zones form the best reservoirs within the Zechstein carbonates on the Utsira High.

This study adds to the understanding of the Zechstein stratigraphy of the northernmost part of the Zechstein Basin. The Utsira High succession evidently was part of the Zechstein Basin fill and shares a comparable depositional history, including early diagenetic overprinting, to the Zechstein successions further south, but has little in common with the Upper Permian succession in East Greenland. The later diagenetic history shares many similarities with the Middle Permian succession in East Greenland, but the timing is different. In East Greenland, calcite replacement occurred during the mid-Permian. On the Utsira High, dedolomitization and dolomite recrystallization occurred during the Triassic – mid-Jurassic and are closely linked to the Mesozoic tectonic and climatic evolution of the area.

The dataset helps to better understand the distribution of porous dolomite reservoirs on the Utsira High and may be useful in future exploration. However, the learnings from the Utsira High may not be directly applicable to other Zechstein shelf successions in the Northern Zechstein Basin, since local tectonics seem to have played a vital role in controlling the diagenetic history and therefore the reservoir quality.

ACKNOWLEDGEMENTS

We thank license partners Aker BP, Equinor and Sval Energy for their approval to publish the presented data. This study is part of the Suprabasins project – Sedimentary response to growth of major extensional fault systems, funded by the Norwegian Research Council (Grant number: 295208), AkerBP, Equinor and Sval Energy. U/Pb dating was undertaken within the frame of a joint research project with the Geological Survey of Norway, funded by Aker BP. We thank Anne-Sophie Cyteval and an anonymous referee for constructive reviews.

REFERENCES

CANAVERAS, J. C., SÁNCHEZ-MORAL, S., CALVO, J. P., HOYOS, M. and ORDÓÑEZ, S., 1996. Dedolomites associated with karstification. An example of early dedolomitization in lacustrine sequences from the Tertiary Madrid basin, central Spain. *Carbonates and Evaporites,* **11**, 85-103.

CLARK, D. N., 1980. The diagenesis of Zechstein carbonate sediments. *Contr. Sedimentology*, **9**, 167-203.

CLARK, D. N., 1986. The Distribution of Porosity in Zechstein Carbonates. In: J. Brooks, J. Goff and B. van Hoorne (Eds), Habitat of Palaeozoic Gas in N.W. Europe. *Geological Society of London, Special Publication* **23**, 121-149. https://doi.org/10.1144/GSL.SP.1986.023.01.09

CLARK, J.A., STEWART, S.A. and CARTWRIGHT, J. A., 1998. Evolution of the NW margin of the North Permian Basin, UK North Sea. *Journal of the Geological Society*, **155**, 663-676.

DANIELS, S.E., TUCKER, M.E., MAWSON, M.J., HOLDSWORTH, R.E., LONG, J.J., GLUYAS J.G. and JONES R. R., 2020. Nature and origin of collapse breccias in the Zechstein of NE England: local observations with cross-border petroleum exploration and production significance, across the North Sea. In: S. Patruno, S. G. Archer, D. Chiarella, J. A. Howell, C. A-L. Jackson and H. Kombrink (Eds), Cross-Border Themes in Petroleum Geology I: The North Sea. *Geological Society of London, Special Publication* **494**, 269-299.

FYFE, J-L. C. and UNDERHILL, J.R., 2023. A regional geological overview of the Upper Permian Zechstein Supergroup (Z1 to Z3) in the SW margin of the Southern North Sea and onshore Eastern England. *Journal of Petroleum Geology,* **46** (3), 223-256.

GLENNIE, K.W., HIGHAM, J. and STEMMERIK, L., 2003. The Permian of the Northern North Sea. In: Evans. D., Graham, C., Armour, A. and Bathurst, P., (Eds), The Millennium Atlas: petroleum geology of the Central and Northern North Sea. London. The Geological Society of London, 91-103.

GRANT, R.J., UNDERHILL, J.R., HERNÁNDEZ-CASADO, J., BARKER, S.M. and JAMIESON, R.J., 2019. Upper Permian Zechstein Supergroup carbonate-evaporite platform palaeomorphology in the UK Southern North Sea. *Marine and Petroleum Geology*, **100**, 484-518.

HILL, C. A., POLYAK, V. J., ASMEROM, Y. and PROVENCIO, P., 2016. Constraints on a Late Cretaceous uplift, denudation, and incision of the Grand Canyon region, southwestern Colorado Plateau, USA, from U-Pb dating of lacustrine limestone. *Tectonics*, **35**(4), 896-906.

JACKSON, C. A.-L., ELLIOTT, G. M., ROYCE-ROGERS, E., GAWTHORPE, R.L. and AAS, T. E., 2019. Salt thickness and composition influence rift structural style, northern North Sea, offshore Norway. *Basin Research,* **31**, 514-538. doi:10.1111/bre.12332

KIERSNOWSKI, H., PAUL, J., PERYT, T. and SMITH, D., 1995. Facies, paleogeography, and sedimentary history of the southern Permian Basin in Europe. In: Scholle, P., Peryt, T. and Ulmer-Scholle, D. (Eds), The Permian of Northern Pangea. Springer Berlin Heidelberg, pp. 119-136. https://doi.org/10.1007/978-3-642-78590-0_7.

OTTESEN, S., SELVIKVÅG, B., SCOTT, A.S.J. MENEGUOLO, R., CULLUM, A., AMILIBIA-CABEZA, A., VIGORITO, M., HELSEM, A. and MARTINSEN, O. J., 2022. Geology of the

Johan Sverdrup field: A giant oil discovery and development project in a mature Norwegian North Sea basin. *AAPG Bulletin*, **106** (4), 897-936. doi:10.1306/11042120037

PATON, C., HELLSTROM, J., PAUL, B., WOODHEAD, J. and HERGT, J., 2011. Iolite: Freeware for the visualisation and processing of mass spectrometric data. *Journal of Analytical Atomic Spectrometry*, **26**, 2508-2518, doi:10.1039/C1JA10172B.

PEGRUM, R. M., 1984. The extension of the Tornquist Zone in the Norwegian North Sea. *Norsk Geologisk Tidsskrift,* **64**, 39-68.

PERYT, T. M., GELUK, M. C., MATHIESEN, A. PAUL, J. and SMITH, K., 2010. Zechstein. In: J.C. Doornenbal and A. G. Stevenson (Eds), Petroleum Geological Atlas of the Southern Permian Basin Area. pp. 123-147. EAGE Publications b.v. (Houten).

PETRUS, J.A., CHEW, D.M., LEYBOURNE, M.I. and KAMBER, B.S., 2017. A new approach to laser-ablation inductively-coupled-plasma mass-spectrometry (LA-ICP-MS) using the flexible map interrogation tool 'Monocle'. *Chemical Geology*, **463**, 76-93, doi:10.1016/j.chemgeo.2017.04.027.

RIBER, L., H. DYPVIK and R. SØRLIE, 2015. Altered basement rocks on the Utsira High and its surroundings, Norwegian North Sea. *Norwegian Journal of Geology*, **95**, 57-89.

RICHTER-BERNBURG, G., 1955. Stratigraphische Gliederung des deutschen Zechsteins. *Zeitschrift der Deutschen Geologischen Gesellschaft,* **105**, 843-854.

RIDER, M.H. and KENNEDY, M., 2011. The Geological Interpretation of Well logs, 3rd Revised edition. Rider-French Consulting Ltd, 440 pp.

ROBERTS, N. M., RASBURY, E. T., PARRISH, R. R., SMITH, C. J., HORSTWOOD, M. S. and CONDON, D. J., 2017. A calcite reference material for LA-ICP-MS U-Pb geochronology. *Geochemistry, Geophysics, Geosystems,* **8**(7), 2807-2814.

SCHOENHERR, J. HALLENBERGER, M., LÜDERS, V., LEMMENS, L., BIEHL, B. C., LEWIN, A., LEUPOLD, M., WIMMERS, K. and STROHMENGER, C. J., 2018. Dedolomitization: review and case study of uncommon mesogenetic formation conditions. *Earth Science Reviews* **185**, 780-805. doi.org/10.1016/j.earscirev.2018.07.005

SCHOLLE, P., STEMMERIK, L. and ULMER, D. S., 1991. Diagenetic History and Hydrocarbon Potential of Upper Permian Carbonate Buildups, Wegener Halvø Area, Jameson Land Basin, East Greenland. *AAPG Bulletin*, **75**, 701-725.

SCHOLLE, P. A., STEMMERIK, L., ULMER-SCHOLLE, D., LIEGRO, G. D. and HENK, F. H., 1993. Palaeokarst influenced depositional and diagenetic patterns in Upper Permian carbonates and evaporites, Karstryggen area, central East Greenland. *Sedimentology*, **40,** 895-918.

SCOTESE, C. R. and LANGFORD, R. P., 1995. Pangea and the Paleogeography of the Permian. In: P. A. Scholle, T. M. Peryt and D. S. Ulmer-Scholle (Eds), The Permian of Northern Pangea, Volume 1: Paleogeography, Paleoclimate, Stratigraphy, pp. 3-19. Springer-Verlag, New York.

SERCK, C.S., BRAATHEN, A., HASSAAN, M., FALAIDE, J. I., RIBER, L., MESSAGER, G. and MIDTKANDAL, I., 2022. From metamorphic core complex to crustal scale rollover: Post-Caledonian tectonic development of the Utsira High, North Sea. *Tectonophysics* **836**, 229416. https://doi.org/10.1016/j.tecto.2022.229416

SŁOWAKIEWICZ, M., BLUMENBERG, M., WIĘCŁAW, D., RÖHLING, H. G., SCHEEDER, G., HINDENBERG, K., LEŚNIAK, A., IDIZ, E. F., TUCKER, M. E., PANCOST, R. D., KOTARBA, M. J. and GERLING, J. P., 2018. Zechstein Main Dolomite oil characteristics in the Southern Permian Basin: I. Polish and German sectors. *Marine and Petroleum Geology*, **93**, 356-375.

SŁOWAKIEWICZ, M., TUCKER, M.E., PANCOST, R.D., PERRI, E. and AWSON, M., 2013. Upper Permian (Zechstein) microbialites: supratidal through deep subtidal deposition, source-rock, and reservoir potential. *AAPG Bull*. **97,** 1921-1936.

SORENTO, T., STEMMERIK, L. and OLAUSSEN, S., 2018. Upper Permian carbonates at the northern edge of the Zechstein Basin, Utsira High, Norwegian North Sea. *Marine and Petroleum Geology* **89**, 635-652.

STEMMERIK, L. and FRYKMAN, P., 1989. Stratigraphy and sedimentology of the Zechstein carbonates of southern Jylland, Denmark. *Danmarks Geologiske Undersøgelse Serie A*, **26,** 33 pp

STENTOFT, N., 1990. Diagenesis of the Zechstein Ca-2 carbonate from the Løgumkloster-1 well, Denmark. *Danmarks Geologiske Undersøgelse Serie B*, **12,** 42 pp.

STROHMENGER, C., ANTONINI, M., JÄGER, G., ROCKENBAUCH, K. and STRAUSS, C., 1996. Zechstein 2 carbonate reservoir facies distribution in relation to Zechstein sequence stratigraphy (Upper Permian, Northwest Germany): An integrated approach. *Bull. Centres Recherches Exploration-Production Elf-Aquitaine,* **20,** 1-35.

TAYLOR, J. C. M., 1998. Upper Permian - Zechstein. In: K. W. Glennie (Ed.), Petroleum Geology of the North Sea: Basic Concepts and Recent Advances, pp. 174-211.

THOMAS, D.W. and COWARD, M. P., 1996. Mesozoic regional tectonics and South Viking Graben formation: evidence for localized thin-skinned detachments during rift development and inversion. *Marine and Petroleum Geology*, **13**, 149-177.

TUCKER, M. E., 1991. Sequence stratigraphy of carbonate-evaporite basins: models and application to the Upper Permian (Zechstein) of northeast England and adjoining North Sea. *Journal of the Geological Society,* **148**, 1019-1036.

VERMEESCH, P., 2018. IsoplotR: A free and open toolbox for geochronology. *Geoscience Frontiers*, **9**, 479-493, doi:10.1016/j.gsf.2018.04.001.

ZIEGLER, P. A., 1990. Permo-Triassic Development of Pangaea. In: P. A. Ziegler (Ed.), Geological Atlas of Western and Central Europe, pp. 68-90. The Hague. Shell International Petroleum Maatsschappij BV.